Soft Matter

PAPER

View Article Online
View Journal | View Issue

Cite this: *Soft Matter*, 2021, 17, 4842

Simple, rapid and sensitive detection of Parkinson's disease related alpha-synuclein using a DNA aptamer assisted liquid crystal biosensor†

Xiuxiu Yang,[a] Xiaofang Zhao,[b] Fengwei Liu,[b] Haiyu Li,[a] Claire Xi Zhang *[b] and Zhongqiang Yang *[a]

Received 26th February 2021,
Accepted 5th April 2021

DOI: 10.1039/d1sm00298h

rsc.li/soft-matter-journal

Alpha-synuclein (αS) has been proposed as a potential biomarker for the diagnosis of Parkinson's disease (PD). However, the detection of αS using a simple, rapid and sensitive approach is still challenging. Herein, we construct a new type of biosensor for the detection of αS, combining the stimuli-responsiveness of liquid crystals (LCs) and the specific interaction of a DNA aptamer with proteins. In principle, the positively charged surfactant hexadecyltrimethylammonium bromide (CTAB) binds with the negatively charged DNA aptamer *via* electrostatic interactions; in the presence of αS, the DNA aptamer specifically binds with αS and releases CTAB, which is an amphiphilic molecule and subsequently assembles at the LC–aqueous interface, resulting in a homeotropic alignment of LCs with a dark optical signal. In the absence of αS, CTAB binds with the DNA aptamer without affecting the alignment of LCs, which shows planar anchoring with a bright optical signal. The response time of LCs towards αS is rapid and can be down to minutes. The LC biosensor established here has a good specificity for αS and can recognize αS even from a mixture of proteins. The LC biosensor also exhibits high sensitivity with a limit of detection of αS as low as 10 pM, which is comparable to that of the enzyme-linked immunosorbent assay. This work provides a new strategy for the detection of αS in a simple, rapid and sensitive manner, possessing promising potentials towards early diagnosis and clinical applications.

Introduction

Parkinson's disease (PD) is the second widespread neurodegenerative disease, especially affecting elderly people.[1,2] At the onset of motor deficits including rigidity, bradykinesia, postural instability, and tremor, patients usually lose more than 60% dopamine neurons in the pars compacta of the substantia nigra.[3] Up to now, PD is not curable; however, the disease progression may be slowed down and suppressed if early diagnosis and intervention are available.[4] SNCA is the first gene linked to familiar PD and its protein product alpha-synuclein (αS) is the central component of Lewy body, one of the major hallmarks of PD pathology.[5,6] In addition, αS is found in body fluids, such as cerebrospinal fluid,[7] blood,[8,9] saliva[10] and tears,[11] making αS a potential biomarker for the early diagnosis of PD. Currently, the detection of αS mainly depends on the enzyme-linked immunosorbent assay.[12] However, it is costly and antibodies may have stability and batch problems. A number of analytical tools such as electrochemical sensors,[13] surface plasmon resonance optical sensors[14] and nanopore-based sensors[15] have been developed for the detection of αS. But these methods are often tedious, time-consuming, and require complex instruments and skilled personnel. Therefore, a simple, rapid and sensitive approach for the detection of αS is still lacking.

Beyond ubiquitous displays, liquid crystals (LCs) with the unique stimuli-responsive properties have become promising analytical candidates for chemical and biological detection.[16–19] In principle, molecular interaction at the interface can disturb LC orientation. This disruption is enlarged to micron level through LCs and transformed into optical signals, thereby achieving a label-free, simple, real-time and zero power detection purpose.[20] So far, LC biosensors have been investigated to report the presence of biological species, such as DNA,[21,22] proteins,[23–26] viruses,[27] bacteria,[28] cells,[29] *etc.* In terms of biomolecular analytics, the specificity and sensitivity of the LC biosensor is critical but still challenging. This is largely because LC itself does not distinguish between targets and other species

[a] *Key Laboratory of Organic Optoelectronics and Molecular Engineering of the Ministry of Education, Department of Chemistry, Tsinghua University, Beijing 100084, China. E-mail: zyang@tsinghua.edu.cn*
[b] *Beijing Institute of Brain Disorders, Laboratory of Brain Disorders, Ministry of Science and Technology, Collaborative Innovation Center for Brain Disorders, Capital Medical University, Beijing 100069, China. E-mail: clairexizhang@ccmu.edu.cn*

† Electronic supplementary information (ESI) available. See DOI: 10.1039/d1sm00298h

present in the aqueous solution. Therefore, in order to impart the LC biosensor with a specific responsiveness to targets, it is necessary to tailor the LC interface, which usually varies from case to case. DNA aptamer is a single stranded DNA sequence which may bind with a specific target ranging from small to big chemical or biological species in a highly specific and sensitive manner.[30] The introduction of a DNA aptamer into LC biosensor has shown its capacity in detecting tumor markers,[31] kanamycin,[32] and reporting aptamer-ligand binding events.[33] Recently, we have established a solid-surface based LC setup to detect αS.[34] Typically, DNA aptamer for αS is anchored to gold substrates. By adding LCs on the aptamer decorated gold substrates, the presence of αS disrupts LC alignment and achieves a label-free detection. This LC biosensor based on LC–solid interface, however, has several limitations of the requirement of fresh and expensive gold coated substrates, multi-step operations, and relatively long detection time (in hours). More importantly, the sensitivity of the biosensor for αS reaches a limit around the concentration of 50 nM, intrinsically restricted by the low density of the DNA aptamer fixed on the substrate. Herein, in order to address these problems, we develop a new and general strategy for the detection of αS. The target protein αS was premixed with the DNA aptamer and amphiphilic surfactant in solution before being directly applied onto the LC interface. The competitive binding of αS with the DNA aptamer released the surfactant and the triggered homeotropic alignment of LCs, causing a dark optical signal. This one-step sensing procedure is simple and straightforward compared to the previous method which involves the preparation of gold coated substrates and multiple steps of incubation, washing and drying. The response of LC interface is instant upon the addition of αS, leading to a much faster and highly sensitive detection.

Experiments

Materials

4-Cyano-4′-pentylbiphenyl (5CB) was obtained from Jiangsu Hecheng Display Technology Co., Ltd (Nanjing, China). Hexadecyltrimethylammonium bromide (CTAB), dimethyloctadecyl [3-(trimethoxysilyl)propyl]ammonium chloride (DMOAP), lysozyme from chicken egg white, α-lactalbumin from bovine milk, thrombin from bovine plasma, α-chymotrypsinogen A from bovine, bovine serum albumin (BSA), phenylmethylsulfonyl fluoride (PMSF), isopropyl-β-D-thiogalactoside (IPTG), Coomassie brilliant blue R, and sodium chloride were purchased from Sigma-Aldrich (USA). Plasmids were bought from Shanghai Heyuan Company (Shanghai, China). Protease inhibitor cocktail (PI) and lysozyme from hen egg white used in the purification of recombinant alpha synuclein (αS) were bought from Roche (Switzerland). Glutathione Sepharose 4B was purchased from GE Healthcare. BL21 (DE3) Chemically Competent Cell (*E. coli*) was obtained from TransGen Biotech (Beijing, China). The buffer solution used in this work was PBS (2 mM KH_2PO_4, 8 mM Na_2HPO_4, 136 mM NaCl and 2.6 mM KCl, pH 7.4). Other salts and solvents were purchased from Sinopharm Chemical Reagents Co., Ltd (Shanghai, China), which were all of analytical grade or above. DNA aptamers were synthesized by Beijing Qingke Biological Technology Co., Ltd (Beijing, China). Gold grids (20 μm thickness, 333 μm pitch, and 55 μm bar width) were purchased from electron microscopy sciences (Fort Washington, PA, USA). Glass microscope slides (Fisher's Finest Premium grade) were obtained from Fisher Scientific (Pittsburgh, PA, USA). Silicone isolators were purchased from Grace Bio-Labs (Bend, OR, USA). The water used in all experiments was Milli-Q water (18.2 MΩ cm). The sequence of DNA aptamer used for αS was: 5′-ATCGAGTGTGTACGGGGTCCGGTAGGGTGGCGAGGTCT TCCTGTCGTAGCAGGATCCA-3′.

Preparation of DMOAP coated glass

The glass slides were functionalized using published procedures.[35] Briefly, the glass slides were first cleaned using piranha solution (70% (v/v) H_2SO_4 and 30% (v/v) H_2O_2). Then, the piranha-cleaned glass slides were coated with 0.5% v/v DMOAP solution in water.

The preparation of recombinant wild-type αS

Recombinant αS was expressed and purified as described before.[36,37]

Preparation of αS fibril

By incubating 2 mg mL^{-1} αS at 37 °C with constant shaking at 1000 rpm (Thermomixer C, Eppendorf) for 7 days, αS fibrils that were micrometers long and tens of nanometers wide in size were prepared. The transmission electron microscopy image of αS fibril is showed in Fig. S3 (ESI†).

Preparation of the optical cells and the liquid crystal (LC) interface

The gold grids were put on the surface of the DMOAP-treated glass. Then, 5CB was dispensed onto each grid. Two silicone isolators (4.5 mm in diameter and 1.7 mm in depth) were placed on the glass slide and pressed to cling to the glass slide. Then, the LC interface was obtained.

Detection of αS

30 μL of 12.5 μM CTAB and 30 μL of 0.75 μM DNA aptamer solution were first mixed and incubated for 20 min at 25 °C. Then, the above solution was mixed with 60 μL of αS solutions with a stated concentration and incubated for 20 min at 25 °C. Finally, 30 μL of the mixed solution was dropped onto the LC–air interface; after 10 min, the optical images were taken. Other proteins were detected by the same procedure.

Optical examination of LC signal

The optical images were examined by using A Nikon Eclipse Ti microscope with a digital camera (Nikon DS-U3) in a transmission mode. Images were captured at a resolution of 1600 × 1200 pixel, a gain of 1.00×, and a shutter speed of 1/30 s.

Results and discussion

The strategy for the detection of αS using the DNA aptamer assisted LC biosensor is illustrated in Fig. 1. Positively charged surfactant hexadecyltrimethylammonium bromide (CTAB) is chosen as it efficiently binds with negatively charged DNA aptamer through electrostatic interaction. In the presence of αS, DNA aptamer preferentially interacts with αS due to higher affinity and releases CTAB. The free amphiphilic CTAB subsequently self-assembles at the LC interface, resulting in a homeotropic LC alignment which exhibits a dark optical signal. In the absence of αS, CTAB binds with the DNA aptamer and fails to assemble at the LC interface, leading to a planar orientation of LCs with a bright optical output.

In this work, nematic LC 4-cyano-4′-pentylbiphenyl (5CB) was confined in a gold grid supported by dimethyloctadecyl [3-(trimethoxysilyl)propyl]ammonium chloride (DMOAP)-treated glass slides. LCs form a homeotropic alignment fixed by the interaction with DMOAP. First, we determined the optimal concentration of CTAB. In an ideal situation, the concentration of CTAB should be as low as possible but still sufficient to allow CTAB to stably assemble at the interface and produce a uniform dark optical signal. Because too much CTAB would electrostatically attract more DNA aptamer and consequently higher amount of αS is needed to competitively bind with DNA aptamer and kick off CTAB. In a typical screening experiment, 30 μL of CTAB in PBS (pH 7.4) was added directly on top of LCs and reached a final concentration of 5 μM, 7.5 μM, 10 μM and 12.5 μM, respectively. After 1 h, as shown in Fig. 2a, the LC sensor gave an all bright optical signal when the concentration of CTAB was 5 μM. With the increase in CTAB concentration from 7.5 μM to 10 μM, CTAB started assembling at the LC interface and inducing a dark optical signal but only in some areas, shown in Fig. 2b and c. When the concentration of CTAB was elevated to 12.5 μM, the stable homeotropic alignment of LCs was generated and stayed uniformly dark under a cross polarized microscope (Fig. 2d). Therefore, the optimal concentration of CTAB for it to stably assemble at the LC–aqueous interface was 12.5 μM in this system and was used in the following experiments.

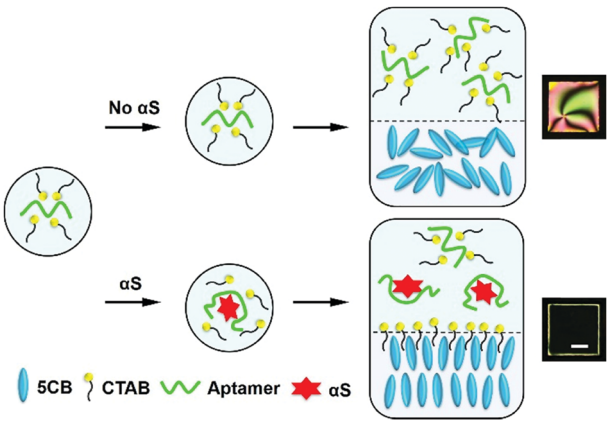

Fig. 1 The schematic illustration of the DNA aptamer assisted LC biosensor for αS detection. The scale bar is 100 μm.

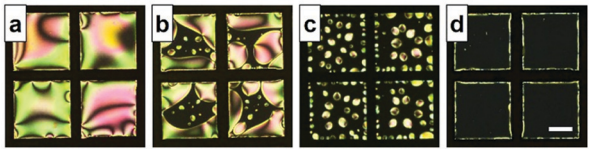

Fig. 2 Optical images (crossed polars) of (a) 5 μM, (b) 7.5 μM, (c) 10 μM and (d) 12.5 μM CTAB assembled LC–aqueous interface for 1 h, respectively. The scale bar is 100 μm.

Next, we determined the optimal concentration of DNA aptamer. Ideally, it is the amount of DNA aptamer that can merely bind with CTAB and prevent CTAB to assemble at the LC interface, resulting in a total bright optical signal. In this case, excessive DNA aptamer is not favorable because these free DNA aptamers will bind with target αS without releasing CTAB, and therefore, the sensitivity of LC biosensor is lowered. In this study, the reported DNA aptamer for αS was used, named F5R1, which is a 58 nt single strand with a K_d of 2.4 nM.[38] For screening DNA aptamer concentration experiment, 30 μL mixture of 12.5 μM CTAB and DNA aptamers with the concentrations of 0.60 μM, 0.65 μM, 0.70 μM and 0.75 μM were added onto the LC interface, respectively. The inspection of Fig. 3 revealed that, after 10 min, with the increase in the DNA aptamer concentration, LCs gradually changed from dark to bright and gave an all bright and stable optical signal at the DNA aptamer concentration of 0.75 μM. This suggested that DNA aptamer at 0.75 μM concentration could prevent the stable assembly of CTAB and lead to a whole bright optical image as desired. In addition, the control experiment showed that 0.75 μM DNA aptamer alone could not induce the LCs to form a homeotropic alignment (Fig. S1, ESI†). These results conclude that the optimal DNA aptamer concentration was 0.75 μM, which was used in the following experiments.

Then, we investigated the detection behavior of the LC biosensor for αS. In a typical experiment, 30 μL mixture solution containing 12.5 μM CTAB, 0.75 μM DNA aptamer and αS ranging from 0 pM to 60 pM was added directly on top of LCs. It usually takes 10 min for optical signals to become stable and then LC images were taken. Fig. 4 shows that when the concentration of αS fell below 10 pM, the interaction between αS and DNA aptamer was insufficient to promote CTAB to be released from the bounded DNA strands; therefore, the orientation of LCs did not show an observable change, retaining the bright optical signal, Fig. 4a and b. Between 10 pM and 15 pM, though naked eyes could hardly distinguish

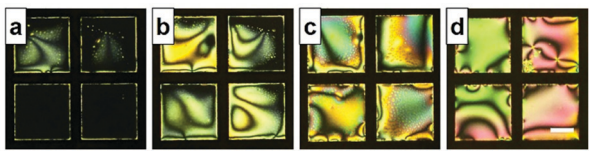

Fig. 3 Optical images (crossed polars) of LC–aqueous interface in the presence of 30 μL mixture of 12.5 μM CTAB and (a) 0.60 μM, (b) 0.65 μM, (c) 0.70 μM, and (d) 0.75 μM DNA aptamer for 10 min, respectively. The scale bar is 100 μm.

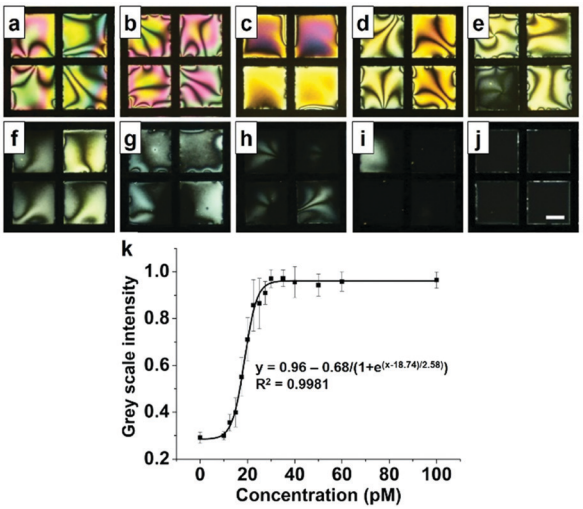

Fig. 4 Optical images (crossed polars) of LC–aqueous interface after adding mixture of 12.5 μM CTAB, 0.75 μM DNA aptamer and (a) 0 pM, (b) 10 pM, (c) 12.5 pM, (d) 15 pM, (e) 17.5 pM, (f) 20 pM, (g) 22.5 pM, (h) 25 pM, (i) 27.5 pM, and (j) 30 pM αS for 10 min, respectively. (k) Relationship between grey scale intensity and concentration of αS. The scale bar is 100 μm.

the little difference among the LC images, with the aid of Matlab (the code is given in the ESI†), we can precisely determine the average grey scale intensity of 9 random selected sample (error bars represent standard deviation), see Fig. 4k. It is reasonably demonstrated that with increase in the αS concentration from 10 pM to 15 pM, the average grey scale intensity continuously increased, *i.e.*, the optical images became darker. Above 15 pM, the optical image in Fig. 4e–i was visually becoming darker, so as the average grey scale intensity gradually increased as shown in Fig. 4k. The optical signal began to turn completely dark when the αS concentration reached 30 pM or above (Fig. 4j and k). This phenomenon indicated that with more and more αS present in the system, the competitive binding between αS and DNA aptamer became dominating and more CTAB was released. Therefore, free CTAB molecules started to assemble at the interface and trigger the orientational change of LCs to the homeotropic alignment, which produced an evident dark optical signal. Examination of Fig. 4j and k also indicated that when αS was above 30 pM, the optical signal became saturated and the average grey scale reached a plateau. This meant the amount of CTAB released at the threshold of 30 pM αS was sufficient to trigger a homeotropic alignment of LCs. Therefore, further increase in the concentration of αS would not cause an additional increase in the average grey scale. Finally, in order to preclude the effect of αS alone on the optical signal of LCs, αS with a concentration of 100 pM was explored. The optical image shown in Fig. S2 (ESI†) stayed bright during the entire period of observation, which indicated that αS under our experimental condition would not induce a homeotropic orientation of LCs or interfere with the optical signal. It is also noted that the operation procedure is easy, only involving mixing and laying the solution on top of LCs. Furthermore, the response time of LCs to αS is rapid, within minutes. Combining these results, it can be concluded that the limit of detection of the LC biosensor for αS can reach as low as 10 pM, which is 5000-fold more sensitive than the former solid surface based LC biosensor. Moreover, the current approach is much simple and faster.

Finally, the selectivity of the LC biosensor was evaluated. As control proteins, αS fibril with a size of several micrometers in length and tens of nanometers in width (Fig. S3, ESI†), BSA, α-chymotrypsinogen A, α-lactalbumin and lysozyme were chosen. Mixture of 12.5 μM CTAB, 0.75 μM DNA aptamer and 100 pM above proteins was directly added on top of the LC interface. After 10 min, the optical signal became stable and was imaged. Fig. 5a–g show that only monomeric αS gave a completely dark optical output, while samples with other proteins or blank control all generated bright images. It was also noted in Fig. 5i that the average grey scale intensity of all other proteins was significantly lower than that of αS. These results indicated that the non-specific interaction between DNA aptamer and control proteins was not sufficient to compete with the interaction between DNA aptamer and CTAB. Therefore, the optical image of LCs stayed bright. It was worth noting that αS fibrils which contained αS but in the aggregated form did not produce a high average grey scale intensity, *i.e.*, the LC biosensor did not respond to αS fibril. This selectivity is attributed to the specificity of the DNA aptamer

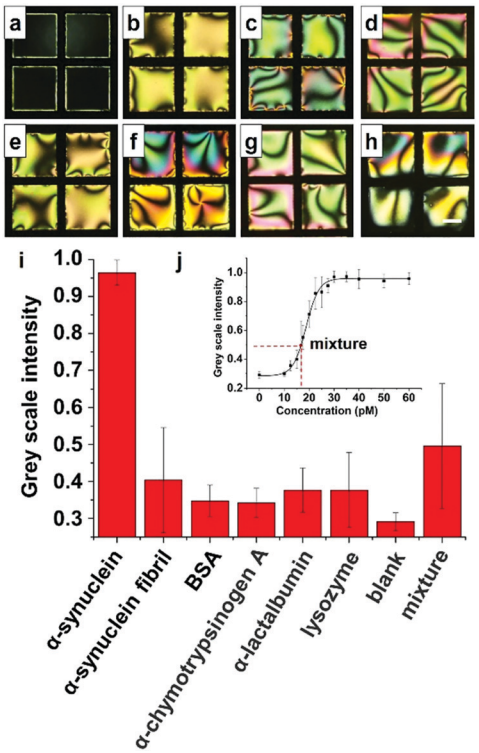

Fig. 5 Optical images (crossed polars) of LC–aqueous interface after adding 12.5 μM CTAB, 0.75 μM DNA aptamer and 100 pM (a) αS, (b) αS fibril, (c) BSA, (d) α-chymotrypsinogen A, (e) α-lactalbumin, (f) lysozyme, (g) blank and (h) mixture of proteins (αS, αS fibril, BSA, α-chymotrypsinogen A, α-lactalbumin and lysozyme at equal ratio), respectively. (i) Grey scale intensity of 100 pM protein either αS, control proteins, blank or mixture. (j) The average grey scale intensity for 100 pM mixture of proteins (αS, αS fibril, BSA, α-chymotrypsinogen A, α-lactalbumin and lysozyme at equal ratio) corresponding to the position of αS grey scale intensity curve. The scale bar is 100 μm.

for αS monomer and not for fibril.[38] Finally, we found that a mixture of proteins at a total concentration of 100 pM, consisting of αS, αS fibril, BSA, α-chymotrypsinogen A, α-lactalbumin and lysozyme at equal ratio, generated a partial dark image as shown in Fig. 5h, and the optical signal located right on the curve of relationship between grey scale intensity and αS concentration, Fig. 5j. While the mixture without αS showed a completely bright optical image and grey scale intensity was lower than that of the mixture solution with αS (Fig. S4, ESI†). These results suggested that the LC biosensor was robust and exhibited high specificity for the detection of αS from a protein mixture.

Conclusions

In this work, we demonstrated a new type of DNA aptamer assisted LC biosensor for the detection of PD related protein, αS. The LC biosensor established here owns several superior advantages: (i) the setup is simple and the materials involved are commercially available, benefiting for the development of disposable sensing kit. (ii) The operation is straightforward, requiring only mixing and pouring the analytes onto LCs. With the aid of a smartphone, the optical signal can be readily imaged and analyzed, making it more user friendly than most other detection methods, which typically need labelling, washing, *etc.*[39,40] (iii) The detection is cost-effective and does not require complex instruments or professional personnel. (iv) The response is rapid, within minutes. This also builds up its foundation for practical use. (v) The LC biosensor can selectively detect target αS even from a mixture of proteins. Additionally, (vi) the LC biosensor has good sensitivity with a detection limit as low as 10 pM, comparable to the now commonly used enzyme-linked immuno-sorbent assay. The level of αS in human plasma and cerebrospinal fluid ranges from 16 pM to 4.5 nM,[12,41] which is just in the detection window of the LC biosensor. This opens up the possibility that the LC biosensor can be not only for clinical but also for home based use and, in the long term, help patients for early diagnosis and treatment. We are also aware of the limitations as the current results were based on an idealized pure substance system. In the application of detection of complex biological samples, this problem can be overcome by simple sample purification. Moreover, αS has been found in saliva[10] and tears,[11] whose composition are much simpler than cerebrospinal fluid and blood, making the LC biosensor a promising analytical approach for those system in future. Additionally, as the aptamer-based LC biosensor exhibits high specificity, it can be potentially applied for screening disease-associated proteins and aggregates. Finally, this LC biosensor provides a general sensing methodology and can be adopted for the detection of a variety of targets and inspires the design and application of analytical tools.[42]

Author contributions

The manuscript was written through contributions of all authors. All authors have given approval to the final version of the manuscript.

Conflicts of interest

There are no conflicts to declare.

Acknowledgements

This work was supported by the National Natural Science Foundation of China (21174077) and Beijing Natural Science Foundation Program and Scientific Research Key Program of Beijing Municipal Commission of Education (KZ201510025023).

Notes and references

1 M. Goedert and A. Compston, *Nat. Rev. Neurol.*, 2018, **14**, 57–62.
2 C. Blauwendraat, M. A. Nalls and A. B. Singleton, *Lancet Neurol.*, 2020, **19**, 170–178.
3 J. B. Schulz and B. H. Falkenburger, *Cell Tissue Res.*, 2004, **318**, 135–147.
4 C. W. Olanow, M. B. Stern and K. Sethi, *Neurology*, 2009, **72**, S1–S136.
5 H. A. Lashuel, C. R. Overk, A. Oueslati and E. Masliah, *Nat. Rev. Neurosci.*, 2013, **14**, 38–48.
6 L. Parnetti, L. Gaetani, P. Eusebi, S. Paciotti, O. Hansson, O. El-Agnaf, B. Mollenhauer, K. Blennow and P. Calabresi, *Lancet Neurol.*, 2019, **18**, 573–586.
7 I. van Steenoven, N. K. Majbour, N. N. Vaikath, H. W. Berendse, W. M. van der Flier, W. D. J. van de Berg, C. E. Teunissen, A. W. Lemstra and O. M. A. El-Agnaf, *Mov. Disord.*, 2018, **33**, 1724–1733.
8 C. W. Chang, S. Y. Yang, C. C. Yang, C. W. Chang and Y. R. Wu, *Front. Neurol. Neurosci.*, 2019, **10**, 1388.
9 R. Pero-Gascon, F. Benavente, Z. Minic, M. V. Berezovski and V. Sanz-Nebot, *Anal. Chem.*, 2020, **92**, 1525–1533.
10 H. Shaheen, S. Sobhy, S. El Mously, M. Abuomira and M. Mansour, *J. Neurol. Psychiatry Neurosurg.*, 2020, **56**, 22.
11 F. Maass, S. Rikker, V. Dambeck, C. Warth, L. Tatenhorst, I. Csoti, M. Schmitz, I. Zerr, A. Leha, M. Bahr and P. Lingor, *Sci. Rep.*, 2020, **10**, 8507.
12 N. K. U. Koehler, E. Stransky, M. Meyer, S. Gaertner, M. Shing, M. Schnaidt, M. S. Celej, T. M. Jovin, T. Leyhe, C. Laske, A. Batra, G. Buchkremer, A. J. Fallgatter, D. Wernet and E. Richartz-Salzburger, *PLoS One*, 2015, **10**, e0123444.
13 Y. An, X. Jiang, W. Bi, H. Chen, L. Jin, S. Zhang, C. Wang and W. Zhang, *Biosens. Bioelectron.*, 2012, **32**, 224–230.
14 A. Khatri, N. Punjabi, D. Ghosh, S. K. Maji and S. Mukherji, *Sens. Actuators, B*, 2018, **255**, 692–700.
15 X. Li, X. Tong, W. Lu, D. Yu, J. Diao and Q. Zhao, *Nanoscale*, 2019, **11**, 6480–6488.
16 N. A. Lockwood, J. K. Gupta and N. L. Abbott, *Surf. Sci. Rep.*, 2008, **63**, 255–293.
17 T. Kato, J. Uchida, T. Ichikawa and T. Sakamoto, *Angew. Chem., Int. Ed.*, 2018, **57**, 4355–4371.
18 Y. K. Kim, J. Noh, K. Nayani and N. L. Abbott, *Soft Matter*, 2019, **15**, 6913–6929.

19 T. Szilvasi, N. Bao, H. Yu, R. J. Twieg, M. Mavrikakis and N. L. Abbott, *Soft Matter*, 2018, **14**, 797–805.
20 Y. Dong and Z. Yang, *Chin. Sci. Bull.*, 2013, **58**, 2557–2562.
21 A. D. Price and D. K. Schwartz, *J. Am. Chem. Soc.*, 2008, **130**, 8188–8194.
22 A. C. McUmber, P. S. Noonan and D. K. Schwartz, *Soft Matter*, 2012, **8**, 4335–4342.
23 J. M. Brake, M. K. Daschner, Y.-Y. Luk and N. L. Abbott, *Science*, 2003, **302**, 2094–2097.
24 D. Hartono, C.-Y. Xue, K.-L. Yang and L.-Y. L. Yung, *Adv. Funct. Mater.*, 2009, **19**, 3574–3579.
25 M. Sadati, A. I. Apik, J. C. Armas-Perez, J. Martinez-Gonzalez, J. P. Hernandez-Ortiz, N. L. Abbott and J. J. De Pablo, *Adv. Funct. Mater.*, 2015, **25**, 6050–6060.
26 I. Pani, P. Madhu, N. Najiya, A. Aayush, S. Mukhopadhyay and S. K. Pal, *J. Phys. Chem. Lett.*, 2020, **11**, 9012–9018.
27 C.-H. Jang, L.-L. Cheng, C. W. Olsen and N. L. Abbott, *Nano Lett.*, 2006, **6**, 1053–1058.
28 S. Sivakumar, K. L. Wark, J. K. Gupta, N. L. Abbott and F. Caruso, *Adv. Funct. Mater.*, 2009, **19**, 2260–2265.
29 N. A. Lockwood, J. C. Mohr, L. Ji, C. J. Murphy, S. P. Palecek, J. J. de Pablo and N. L. Abbott, *Adv. Funct. Mater.*, 2006, **16**, 618–624.
30 G. Mayer, *Angew. Chem., Int. Ed.*, 2009, **48**, 2672–2689.
31 L. Qi, S. Liu, Y. Jiang, J. M. Lin, L. Yu and Q. Hu, *Anal. Chem.*, 2020, **92**, 3867–3873.
32 Y. Wang, B. Wang, J. Shen, X. Xiong and S. Deng, *Microchim. Acta*, 2017, **184**, 3765–3771.
33 P. S. Noonan, R. H. Roberts and D. K. Schwartz, *J. Am. Chem. Soc.*, 2013, **135**, 5183–5189.
34 X. Yang, H. Li, X. Zhao, W. Liao, C. X. Zhang and Z. Yang, *Chem. Commun.*, 2020, **56**, 5441–5444.
35 X. Yang, Y. Tian, F. Li, Q. Yu, S. F. Tan, Y. Chen and Z. Yang, *Langmuir*, 2019, **35**, 2490–2497.
36 N. K. Polinski, L. A. Volpicelli-Daley, C. E. Sortwell, K. C. Luk, N. Cremades, L. M. Gottler, J. Froula, M. F. Duffy, V. M. Y. Lee, T. N. Martinez and K. D. Dave, *J. Parkinson's Dis.*, 2018, **8**, 303–322.
37 Y. Guan, X. Zhao, F. Liu, S. Yan, Y. Wang, C. Du, X. Cui, R. Li and C. X. Zhang, *Front. Cell. Neurosci.*, 2020, **14**, 159.
38 Y. Zheng, J. Qu, F. Xue, Y. Zheng, B. Yang, Y. Chang, H. Yang and J. Zhang, *Mol. Ther.–Nucleic Acids*, 2018, **11**, 228–242.
39 R. Nandi and S. K. Pal, *Analyst*, 2018, **143**, 1046–1052.
40 Y.-C. E. Li and I. C. Lee, *Biosensors*, 2020, **10**, 88.
41 L. M. Chahine, T. G. Beach, M. C. Brumm, C. H. Adler, C. S. Coffey, S. Mosovsky, C. Caspell-Garcia, G. E. Serrano, D. G. Munoz, C. L. White, J. F. Crary, D. Jennings, P. Taylor, T. Foroud, V. Arnedo, C. M. Kopil, L. Riley and K. D. Dave, *Neurology*, 2020, **95**, e1267–e1284.
42 Y. Zhang, B. S. Lai and M. Juhas, *Molecules*, 2019, **24**, 941.